Polygonal shape transformation of a circular biconcave vesicle induced by osmotic pressure

Hiroyoshi Naito and Masahiro Okuda
Department of Physics and Electronics, Osaka Prefecture University, Gakuen-cho, Sakai, Osaka 593, Japan

Ou-Yang Zhong-can
Institute of Theoretical Physics, Academia Sinica, P.O. Box 2735 Beijing 100080, China
(Received 13 June 1994; revised manuscript received 10 July 1995)

Polygonal shape transformation processes observed in liposomes [H. Hotani, J. Mol. Biol. **178**, 113 (1984)] have been analyzed on the basis of the Helfrich spontaneous curvature model. First, a mathematical solution for the biconcave axisymmetric vesicles [H. Naito, M. Okuda, and Z. Ou-Yang, Phys. Rev. E **47**, 2304 (1993)] is derived, and then the second variation of the shape energy of the slightly deformed vesicles from the biconcave shape is calculated. After the minimization of the shape energy, it is found that the biconcave vesicle is transformed into elliptical, triangular, square, pentagonal, or other polygonal shapes above the threshold osmotic pressure difference. At a constant value of $\Delta V/V_0$, the osmotic pressure is found to be a monotonic increasing function of m, except for $m=2$, where V_0 is the initial volume of the biconcave vesicle, ΔV is the change in the volume of the deformed vesicle, and m denotes mth polygonal deformation. It is shown that the experimental results of the polygonal shape transformation in liposomes can be well explained by the present theoretical predictions. [S1063-651X(96)09909-6]

PACS number(s): 87.22.Bt, 82.65.−i, 68.15.+e, 46.30.−i

I. INTRODUCTION

Recently, both experimental and theoretical aspects of amphiphile bilayers and monolayers have gathered much attention from physicists and chemists [1]. Amphiphilic molecules, such as phospholipids, are often assembled into bilayers that form single shells called vesicles because of the repulsive interaction between the hydrocarbon chains of lipid and water molecules. These structures are regarded as simple models for biomembranes and cells [2–5]. A great success in this field is the understanding of the role of the bending elasticity for both equilibrium shapes and their fluctuations of fluid membranes [1].

The shape transformations of the vesicles can be induced by changing external parameters, such as temperature [6] and osmotic pressure [7]. One of the most interesting problems in this context is the transformation pathways of liposomes reported by Hotani [7]. He has shown with the dark-field microscope that liposomes whose initial shapes are circular biconcave transform into elliptical, triangular, square, or pentagonal shapes, as schematically illustrated in Fig. 1, and has concluded that the driving force for the transformations is osmotic pressure. Since these transformation pathways have also been found in biological membrane vesicles, such as vesicles derived from human red blood cell (RBC) ghosts after digestion of surface membrane proteins by trypsin, the transformation is a general intrinsic property of lipid membranes and hence is a theoretically important issue.

Sekimura and Hotani [8] have numerically explained the shape transformation pathways on the basis of the Canham model, which does not include spontaneous curvature [9]. However, their approach has two principal weak points. First, the Canham model predicts two shapes having the same minimum energy, a dumbbell-like shape and a biconcave shape; the former shape has not been found in RBCs [2]. Second, a modified Cassini equation was employed as the initial biconcave shape, but is apparently different from the real biconcave shape of RBCs [10]. To overcome the first weak point, Helfrich [11] has shown the importance of spontaneous curvature and has developed a phenomenological theory for the elasticity of fluid membranes by analogy with the curvature elasticity of liquid crystals. The spontaneous curvature in this model likely results from the asymmetric molecular distribution between the inner and the outer monolayer of membranes. Deuling and Helfrich have shown that

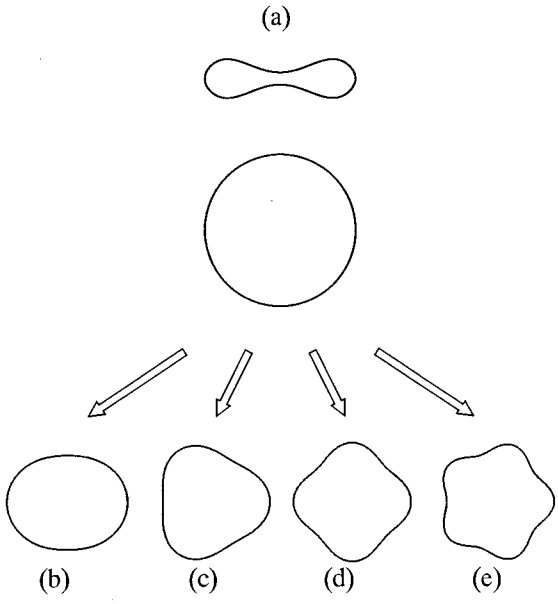

FIG. 1. Schematic illustration of polygonal shape transformation pathways of liposomes by osmotic dehydration [7]. The liposomes having circular biconcave shape whose side and top views are shown in (a) are transformed into (b) elliptical, (c) triangular, (d) square or (e) pentagonal shapes.

the RBCs under normal physiological conditions have negative spontaneous curvature [12]. Since this model has been widely used for the study of amphiphile monolayers and bilayers [4], the theoretical analysis of the polygonal shape transition should be based on the Helfrich spontaneous curvature model. The theoretical analysis has already been carried out by Kawakatsu, Andelman, Kawasaki, and Taniguchi [13]. They numerically studied polygonal shapes of vesicles having two component membranes, and their calculation was based on the shape equation by Seifert, Berndl, and Lipowsky [14], which is different from the shape equation derived from the Helfrich model [15].

In this paper, we apply the Helfrich spontaneous curvature model to the analysis of the shape transformation of liposomes having the polygonal symmetry observed by Hotani [7]. In Sec. II, using the shape equation for the axisymmetric vesicles derived originally by Hu and Ou-Yang [15], an analytical solution to the shape equation [15] is derived under the conditions of no surface tension and no osmotic pressure difference, which have been derived from the fundamental principle of surface chemistry for phospholipid vesicles in an aqueous medium [16]. It is demonstrated that the solution is a circular biconcave discoid in the case of negative spontaneous curvature. Hence, the biconcave solution is suitable for the initial shape of the polygonal shape transformation. Section III presents the calculation of the second variation of the shape energy of the vesicle having slight distortion from the initial biconcave solution using the general formula for the stability analysis of equilibrium shape given by Ou-Yang and Helfrich [17]. Section IV derives and solves the Euler-Lagrange equation for the second variation formula in the polygonal deformation mode. Section V discusses the present theoretical results. It is found that the theoretical results are in good agreement with those of the experiment. Section VI concludes the article.

II. A SOLUTION FOR BICONCAVE VESICLES

In the Helfrich spontaneous curvature model, the equilibrium shape of a vesicle is determined by the minimization of the shape energy, which is

$$F=(k/2)\oint (c_1+c_2-c_0)^2 dA+\Delta p\int dV+\lambda\oint dA, \tag{2.1}$$

where k, c_1 and c_2, and c_0 are the bending rigidity, the two principal curvatures and the spontaneous curvature, respectively. Since we consider the vesicles with spherical topology here, the additional Gaussian curvature energy term $k\oint c_1c_2dA$ in the original expression of the bending energy [11] is equal to $4\pi k$ and has been neglected in Eq. (2.1), where k is the Gaussian curvature modulus. The second and third terms in Eq. (2.1) either take into account the constraints of constant volume and area or represent actual work. Depending on the considered situation, the two parameters Δp and λ serve as Lagrange multipliers or the actual osmotic pressure difference between outer and inner media ($\Delta p=p_{\rm out}-p_{\rm in}$) and the tensile stress, respectively.

Instead of the spontaneous curvature, the bilayer couple model [18] introduced the constraint of the area difference between outer and inner monolayers of a membrane by $\gamma\Delta A$, where γ is an additional Lagrange multiplier. However, the simple derivation [see Eq. (19) in Ref. [17]] shows that for a uniform membrane the area difference ΔA can always be written as

$$\Delta A=\oint [t(c_1+c_2)+t^2c_1c_2]dA+O(t^3), \tag{2.2}$$

where t is the thickness of the bilayer. It is evident that the $\gamma\Delta A$ term can be incorporated in the c_0 and k values in Eq. (2.1). Thus we should stress that the bilayer couple model is essentially identical to the Helfrich spontaneous curvature model.

Since the Helfrich shape energy, Eq. (2.1), is a complete combination of linear and quadratic invariants of the surface curvatures c_1 and c_2, the minimization of Eq. (2.1) generates a variety of surfaces in the Euclidean space. For the description of such surfaces, a general shape equation of equilibrium vesicles has been derived from the first variation of Eq. (2.1) by using general rules of differential geometry and imposing the closed condition of the surface of vesicles, and is

$$\Delta p-2\lambda H+k(2H+c_0)(2H^2-2K-c_0H)+2k\nabla^2H=0, \tag{2.3}$$

where $K=c_1c_2$ and $H=(-1/2)(c_1+c_2)$ are the Gaussian and the mean curvatures, respectively, and ∇^2 is the Laplace-Beltrami operator [19].

Only axisymmetric equilibrium shapes of vesicles have been extensively studied with numerical methods so far [14,20]. In this study, we use the general shape equation for axisymmetric vesicles that has been derived from Eq. (2.3) by Hu and Ou-Yang [15] and that is a third-order differential equation of $\psi(\rho)$,

$$\begin{aligned}\cos^3\psi\left(\frac{d^3\psi}{d\rho^3}\right)=&4\sin\psi\cos^2\psi\left(\frac{d^2\psi}{d\rho^2}\right)\left(\frac{d\psi}{d\rho}\right)-\cos\psi\Bigg(\sin^2\psi\\&-\frac{1}{2}\cos^2\psi\Bigg)\left(\frac{d\psi}{d\rho}\right)^3+\frac{7\sin\psi\cos^2\psi}{2\rho}\left(\frac{d\psi}{d\rho}\right)^2\\&-\frac{2\cos^3\psi}{\rho}\left(\frac{d^2\psi}{d\rho^2}\right)+\left[\frac{c_0^2}{2}-\frac{2c_0\sin\psi}{\rho}+\frac{\lambda}{k}\right.\\&\left.-\frac{\sin^2\psi-2\cos^2\psi}{2\rho^2}\right]\cos\psi\left(\frac{d\psi}{d\rho}\right)\\&+\left[\frac{\Delta p}{k}+\frac{\lambda\sin\psi}{k\rho}+\frac{c_0^2\sin\psi}{2\rho}\right.\\&\left.-\frac{\sin^3\psi+2\sin\psi\cos^2\psi}{2\rho^3}\right],\end{aligned} \tag{2.4}$$

where ρ is the distance from the symmetric axis (z axis) of rotation, $\psi(\rho)$ is the angle made by the surface tangent, and the ρ axis as shown schematically in Fig. 2. In this case, we have the following relations:

$$\frac{dz}{ds}=\sin\psi \tag{2.5}$$

and

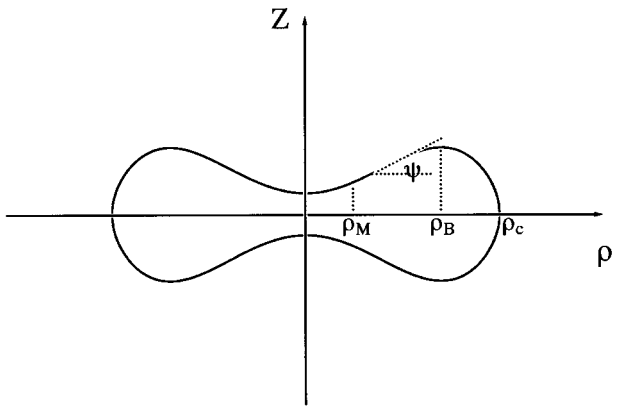

FIG. 2. Schematic illustration of a cross section of a vesicle with $D_{\infty h}$ symmetry. The z axis is the axis of rotational symmetry.

$$\frac{d\rho}{ds}=\cos\psi, \tag{2.6}$$

where s is the arc length of the vesicle with axisymmetry. The vesicle surface is hence represented by the vector $\vec{Y}(s,\phi)$ in Euclidean space as

$$\vec{Y}(s,\phi)=(\rho(s)\cos\phi,\rho(s)\sin\phi,z(s)), \tag{2.7}$$

where ϕ is the azimuthal angle. Once $\psi(\rho)$ is solved from Eq. (2.4), we can obtain the contour $z(\rho)$ $[=z(s)]$ by a simple integration,

$$z(\rho)-z(0)=\int_0^\rho \tan\psi(\rho')d\rho'. \tag{2.8}$$

Note that there exist two branches of $\psi(\rho)$ for vesicles with C_∞ symmetry, which are the upper and the lower branches with respect to the equatorial plane that contains the ρ axis, while for vesicles with $D_{\infty h}$ symmetry, such as biconcave and dumbbell-like shapes, these two branches are identical. We study the latter case in this section.

Since the biconcave liposomes begin to deform with increasing osmotic pressure difference [7], it is reasonable to assume that the initial biconcave vesicles exist at

$$\Delta p=\lambda=0. \tag{2.9}$$

This constraint is indeed an important condition required from surface chemistry as well as serving to simplify Eq. (2.4). Tanford has pointed out that for phospholipid vesicles formed from neutral lipid molecules in pure water, the pressures on the two sides of the vesicle membranes must be exactly equal, i.e., $\Delta p=0$, because the membranes are permeable to water [16]. Tanford has shown further that in a symmetric bilayer bounded on both sides by water, the surface area of the bilayer adjusts itself to its optimal value at $(\partial F/\partial A)_{T,V}=0$, and hence the surface tension vanishes, i.e., $\lambda=0$. Condition (2.9) is also based on the consideration by Brochard and Lennon [21] that the normal state of RBCs can be characterized by no surface tension, no pressure difference, and finite curvature energy. Furthermore, de Gennes has emphasized that $\lambda=0$ is a good approximation for RBCs [22]. In addition, Deuling and Helfrich have shown from the numerical calculation for axisymmetric vesicles [20] that the sign of Δp is either positive (the upper figure of Fig. 3 in their article) or negative (the right figure of Fig. 12) for biconcave discoids. Thus we can expect that a biconcave discoid with $\Delta p=0$ does exist. From these reasons, we focus our attention on the general solutions of Eq. (2.4) under condition (2.9) in the following and show that the circular biconcave shape is a solution of Eq. (2.4).

Although Eq. (2.4) cannot be greatly reduced, even using Eq. (2.9), surprisingly we can find an analytic solution of Eq. (2.4),

$$\psi=\arcsin[\rho(c_0\ln\rho+b)], \tag{2.10}$$

where b is a constant dependent on the size of the vesicle. The proof of Eq. (2.10) is straightforward and can be carried out by substituting the first, second, and third differentiation of ψ with respect to ρ, which are

$$\frac{d\psi}{d\rho}=\frac{1}{\cos\psi}\left(\frac{\sin\psi}{\rho}+c_0\right), \tag{2.11}$$

$$\frac{d^2\psi}{d\rho^2}=\frac{\sin\psi}{\cos^3\psi}\left(\frac{\sin\psi}{\rho}+c_0\right)^2+\frac{c_0}{\rho\cos\psi}, \tag{2.12}$$

and

$$\frac{d^3\psi}{d\rho^3}=\left(\frac{3\sin^2\psi}{\cos^5\psi}+\frac{1}{\cos^3\psi}\right)\left(\frac{\sin\psi}{\rho}+c_0\right)^3 + \frac{3c_0\sin\psi}{\rho\cos^3\psi}\left(\frac{\sin\psi}{\rho}+c_0\right)-\frac{c_0}{\rho^2\cos\psi}, \tag{2.13}$$

respectively, into Eq. (2.4) with the condition, Eq. (2.9).

As pointed out in our previous paper [23], the solution represents a circular biconcave shape in case of negative spontaneous curvature. We describe here the characteristics of the solution in detail. From the equation,

$$\frac{dz}{d\rho}=\tan\psi=\rho(c_0\ln\rho+b)/\cos\psi=0, \tag{2.14}$$

we find two extrema of $z(\rho)$ that are located at $\rho=0$ and

$$\rho=\rho_B=\exp[-b/c_0]. \tag{2.15}$$

Then the solution is rewritten as

$$\psi=\arcsin[\rho c_0\ln(\rho/\rho_B)]. \tag{2.16}$$

Using Eq. (2.16), Eq. (2.11) is also rewritten as

$$\frac{d\psi}{d\rho}=\frac{c_0[\ln(\rho/\rho_B)+1]}{\cos\psi}. \tag{2.17}$$

Because of $c_0<0$, $d\psi/d\rho=0$ yields the maximum value for ψ,

$$\psi=\psi_m=\arcsin(-\rho_M c_0), \tag{2.18}$$

at

$$\rho=\rho_M=\rho_B/e, \tag{2.19}$$

where $\ln e=1$. From $0<\psi_m<\pi/2$, the range of $\rho_B c_0$ is

$$0>\rho_B c_0 \geqslant -e. \tag{2.20}$$

At the equator of a vesicle with $D_{\infty h}$ symmetry, as shown in Fig. 2, ψ is equal to $-\pi/2$. Substituting $\psi=-\pi/2$ into Eq. (2.16), we find the relation between ρ_B and the equatorial radius ρ_c,

$$\rho_c c_0 \ln(\rho_c/\rho_B)=-1. \tag{2.21}$$

From Eqs. (2.19)–(2.21), we have $0<\rho_M<\rho_B<\rho_c$.

The behavior of the solution, Eq. (2.10), becomes obvious from the above description. From $\rho=0$ to ρ_M, ψ monotonically increases from 0 to ψ_m, and from ρ_M to ρ_c, ψ monotonically decreases from ψ_m to $-\pi/2$ and changes its sign from positive to negative at $\rho=\rho_B$. Accordingly, $z(\rho)$ in Eq. (2.8) monotonically increases from $\rho=0$ to ρ_B, takes the maximum value at $\rho=\rho_B$, and then monotonically decreases from ρ_B to ρ_c. The schematic contour of $z(\rho)$ can be seen in one quadrant of Fig. 2. We note that Eq. (2.10) does describe a circular biconcave shape in case of $c_0<0$, together with an appropriate ρ_B value in the range determined from Eqs. (2.20) and (2.21) and

$$\int_0^{\rho_c} \tan\psi(\rho')d\rho'<0, \tag{2.22}$$

which is from $z(0)>z(\rho_c)$. The above analysis indicates that under the constraints of Eqs. (2.19)–(2.21) the shapes generated by the solution are uniquely determined by c_0 and ρ_B. Instead of ρ_B, the shapes are also determined by c_0 and the vesicle surface area A_0, because we have the following relation between A_0 and ρ_B:

$$A_0=4\pi\int_0^{\rho_c}\frac{\rho}{\sqrt{1-[\rho c_0\ln(\rho/\rho_B)]^2}}\,d\rho. \tag{2.23}$$

We choose the biconcave shape as an initial shape for the study of the polygonal shape transition. This choice is more reasonable than that of a modified Cassini equation in Ref. [8]. Since the shape transformation has been observed in vesicles derived from human RBC ghosts after digestion of surface membrane proteins by trypsin as well as in liposomes, we fit the biconcave shape to the human RBC shape. To do this, we employ the experimentally obtained shape equation for human RBCs by Evans and Fung [10],

$$z(\rho)=\frac{1}{2}\sqrt{1-\left(\frac{\rho}{\rho_c}\right)^2}\left[A+B\left(\frac{\rho}{\rho_c}\right)^2+C\left(\frac{\rho}{\rho_c}\right)^4\right], \tag{2.24}$$

where $\rho_c=3.91$ μm, $A=0.81$ μm, $B=7.8$ μm, and $C=-4.39$ μm. The shape is shown in Fig. 3 by a solid line. This shape possesses a maximum of $z(\rho)=1.28$ μm at $\rho_B=0.70\rho_c$. We fit the shape of the present solution Eq. (2.16) to Eq. (2.24) at $\rho_c=3.91$ μm, and obtain $\rho_B=0.62\rho_c$ and $c_0R_0=-1.67$, where $R_0=\sqrt{A_0/4\pi}$ and $A_0=126$ μm^2. The best-fitted curve is also shown in Fig. 3 by a dotted line, and is in good agreement with the experimental RBC shape in whole range from $\rho=0$ to $\rho=\rho_c$, but with slight deviation. The deviation does not have a serious meaning in principle,

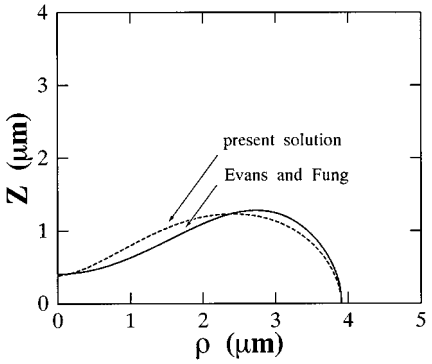

FIG. 3. Cross section of cell shapes. Only one quadrant is shown. There is rotational symmetry around the z axis and reflection symmetry at the ρ axis. Solid line represents the experimentally obtained expression for RBCs by Evans and Fung [10]. Dashed line represents Eq. (2.16), the solution to Eq. (2.4) with $\rho_c=3.91$ μm, $\rho_B/\rho_c=0.62$ and $c_0R_0=-1.67$.

because Evans and Fung's experimental expression represents an averaged shape over 50 RBCs, and indeed, a RBC with the same shape as the present theoretical result has been observed (see, for example, Cell 2 in Ref. [24]). Furthermore, the c_0R_0 value deduced here agrees well with $c_0R_0=-1.62$, which has been obtained from the three geometric relations for vesicles using Eq. (2.24) as an approximate shape solution for the RBC shape [25]. It is therefore reasonable to use the present theoretical shape, Eq. (2.16), with $\rho_B=0.62\rho_c$ and $c_0=-0.53$ μm^{-1} as the initial shape for the polygonal shape transformation.

III. SECOND VARIATION OF THE BICONCAVE VESICLES

As described previously, we assume that the initial shape of the vesicle is the circular biconcave shape defined by Eqs. (2.8), (2.9), and (2.16) with the fixed values of c_0, ρ_B, and ρ_c. It has been reported that the membrane area is constant, while the membrane volume is decreased during the polygonal shape transformation of liposomes [7]. Thus λ and Δp in Eq. (3.2) are regarded, respectively, as a Lagrange multiplier and an actual osmotic pressure difference, which is the driving force for the transformation [7], and have small nonzero values, because these two quantities are related to each other [see Eq. (4.24)]. Of course, the vesicle shape can also be deformed by changing spontaneous curvature; however, to examine the effect of osmotic pressure difference, we assume that c_0 is constant in the present calculation. This assumption is reasonable because the circular biconcave form of the side view was maintained during the polygonal shape transformation processes of liposomes [7].

We consider a slightly deformed surface defined as

$$\vec{Y}'=\vec{Y}+q(s,\phi)\vec{n}, \tag{3.1}$$

where $\vec{n}$ is the outward unit vector normal to the initial surface of the biconcave vesicle $\vec{Y}(s,\phi)$, and $q(s,\phi)$ is a sufficiently small and smooth function. Accordingly, from Eq. (2.1), the shape energy of a deformed vesicle, which is expanded up to second order with respect to q, is

$$F=F_b^{(0)}+\delta^{(1)}F_b+\delta^{(2)}F_b+\Delta pV_0+\Delta p(\delta^{(1)}V+\delta^{(2)}V)$$
$$+\lambda A_0+\lambda(\delta^{(1)}A+\delta^{(2)}A), \tag{3.2}$$

where $F_b^{(0)}$, V_0, and A_0 are the bending energy, volume, and area of the initial biconcave vesicle, respectively, and $\delta^{(1)}$ and $\delta^{(2)}$ correspond to the first and the second variations, respectively.

For the calculation of the quantities on the right-hand side of Eq. (3.2), the most straightforward and convenient approach has been shown by Ou-Yang and Helfrich [17]; they have derived the general expressions for the first and the second variations of the shape energy. By putting the general coordinates $u=s$ and $v=\phi$, and using Eqs. (2.5)–(2.7) and Eqs. (2) and (3) in Ref. [17], we have the following geometric quantities of the initial vesicle:

$$\vec{Y}_1=\partial_s\vec{Y}=(\cos\psi\cos\phi,\cos\psi\sin\phi,\sin\psi),$$
$$\vec{Y}_2=\partial_\phi\vec{Y}=(-\rho\sin\phi,\rho\cos\phi,0),$$
$$g_{11}=\vec{Y}_1\cdot\vec{Y}_1=1,\quad g_{12}=\vec{Y}_1\cdot\vec{Y}_2=0,\quad g_{22}=\vec{Y}_2\cdot\vec{Y}_2=\rho^2,$$
$$g=\det(g_{ij})=\rho^2,$$
$$\vec{n}=\vec{Y}_1\times\vec{Y}_2/\sqrt{g}=(-\sin\psi\cos\phi,-\sin\psi\sin\phi,\cos\psi). \tag{3.3}$$

From Eqs. (2.6) and (2.11) we also have

$$\frac{d\psi}{ds}=\frac{d\psi}{d\rho}\frac{d\rho}{ds}=\left(\frac{\sin\psi}{\rho}+c_0\right). \tag{3.4}$$

From Eqs. (3.3) and (3.4), the second fundamental forms of the surface are

$$L_{11}=\vec{n}\cdot\partial_s^2\vec{Y}=\frac{\sin\psi}{\rho}+c_0,$$
$$L_{12}=\vec{n}\cdot\partial_s\partial_\phi\vec{Y}=L_{21}=0,$$
$$L_{22}=\vec{n}\cdot\partial_\phi^2\vec{Y}=\rho\sin\psi. \tag{3.5}$$

Since $g_{12}=L_{12}=0$, $g^{11}=g_{11}^{-1}$, $g^{22}=g_{22}^{-1}$, $L^{11}=L_{11}^{-1}$, and $L^{22}=L_{22}^{-1}$, the mean and the Gaussian curvatures can be obtained as

$$H=\tfrac{1}{2}g^{ij}L_{ij}=\frac{\sin\psi}{\rho}+\frac{c_0}{2} \tag{3.6}$$

and

$$K=\frac{\sin\psi}{\rho}\left(\frac{\sin\psi}{\rho}+c_0\right), \tag{3.7}$$

respectively. The Christoffel symbols Γ_{ij}^k defined by [26]

$$\Gamma_{ij}^k=\tfrac{1}{2}g^{kl}(\partial_i g_{lj}+\partial_j g_{li}-\partial_l g_{ij}) \tag{3.8}$$

also appear in the general formula for the second variation of the shape energy [see Eq. (39) in Ref. [17]]. Substituting Eq. (3.3) into (3.8), we have

$$\Gamma_{11}^1=\Gamma_{11}^2=\Gamma_{12}^1=\Gamma_{22}^2=0,$$
$$\Gamma_{22}^1=-\rho\cos\psi,\quad \Gamma_{12}^2=\frac{\cos\psi}{\rho}. \tag{3.9}$$

These results can easily be checked in case of spherical vesicles. As shown in our previous paper [23], let $c_0=0$ and $b=1/R_0$; Eq. (2.10) becomes $\rho=R_0\sin\psi$, which represents a sphere with radius R_0. Substituting $\rho=R_0\sin\psi$ into Eq. (3.9) yields the same expressions of the Christoffel symbols for the sphere as Eq. (42) in Ref. [17], if we set $R_0=1$. This is because the general coordinate $u=\theta=\psi$ and $v=\phi$ was used in Ref. [17], whereas $u=s=R_0\psi$ and $v=\phi$ in the present paper for the sphere. We can now calculate all the terms in Eq. (3.2).

The first term on the right-hand side of Eq. (3.2), $F_b^{(0)}$, is given by that of Eq. (2.1). However, we do not deduce $F_b^{(0)}$, because we are interested in the variation of the shape energy, $\delta F=F-F_b^{(0)}$. The second term in Eq. (3.2), the first variation of the shape energy $\delta^{(1)}F_b$, is zero, because the biconcave vesicle, Eq. (2.10), is an equilibrium shape under the condition of $\Delta p=\lambda=0$. The third term, the second variation of the energy $\delta^{(2)}F_b$, is [see Eq. (39) in Ref. [17]]

$$\delta^{(2)}F_b=\oint(q^2[2k(H+c_0/2)(8H^3-5KH+c_0K/2)$$
$$+2k(K-2H^2)(K+2c_0H+2H^2)$$
$$+2(k/\sqrt{g})\partial_i\partial_j[\sqrt{g}(H+c_0/2)(2Hg^{ij}-KL^{ij})]$$
$$-(k/\sqrt{g})\partial_m\{\sqrt{g}(H+c_0/2)[g^{ij}\partial_j(L_{jl}g^{lm})$$
$$-L_{lk}g^{km}g^{ij}\Gamma_{ij}^l-(2Hg^{ij}-KL^{ij})\Gamma_{ij}^m]\}]$$
$$+q_iq_j\{k(H+c_0/2)^2g^{ij}+2k(H+c_0/2)$$
$$\times(KL^{ij}-3Hg^{ij})\}-2k(K+c_0H)qg^{ij}\nabla_iq_j$$
$$+(k/2)(g^{ij}\nabla_iq_j)^2)dA, \tag{3.10}$$

where $q_i=\partial_iq$ and ∇_iq_i is the covariant derivative of q_i defined by

$$\nabla_iq_j=\partial_i\partial_jq-\Gamma_{ij}^kq_k. \tag{3.11}$$

After some calculation, we have

$$\delta^{(2)}F_b=k\oint[q^2c_0^4(2c_0^{-2}\rho^{-2}-2x^3-4x^2+\tfrac{1}{2})$$
$$+q_s^2c_0^2(\tfrac{1}{2}c_0^{-2}\rho^{-2}-x^2-\tfrac{1}{2}x-1)$$
$$+q_\phi^2c_0^4(c_0^{-2}\rho^{-2}-2c_0^{-4}\rho^{-4})$$
$$+\tfrac{1}{2}q_{ss}^2+\tfrac{1}{2}q_{\phi\phi}^2\rho^{-4}+q_{s\phi}^2\rho^{-2}]dA, \tag{3.12}$$

where $x=\ln(\rho/\rho_B)$, $q_s=\partial_sq$, $q_\phi=\partial_\phi q$, $q_{ss}=\partial_s^2q$, $q_{\phi\phi}=\partial_\phi^2q$, and $q_{s\phi}=\partial_s\partial_\phi q$.

The other important terms in Eq. (3.2) are the area and the volume variations, which are [see Eqs. (19) and (20) in Ref. [17]]

$$\delta A=\oint(-2Hq+\tfrac{1}{2}g^{ij}q_iq_j+Kq^2)dA \tag{3.13}$$

and

$$\delta V = \oint (q - Hq^2) dA, \tag{3.14}$$

respectively. Using Eqs. (3.3), (3.6), and (3.7), we reduce these two equations to

$$\Delta p(\delta^{(1)}V + \delta^{(2)}V) = \Delta p \oint [q - c_0(x+\tfrac{1}{2})q^2] dA \tag{3.15}$$

and

$$\lambda(\delta^{(1)}A + \delta^{(2)}A) = \lambda \oint [-2c_0(x+\tfrac{1}{2})q + \tfrac{1}{2}(q_s^2 + \rho^{-2}q_\phi^2) + c_0^2 x(x+\tfrac{1}{2})q^2] dA. \tag{3.16}$$

Substituting Eqs. (3.12), (3.15), (3.16), and $\delta^{(1)}F_b = 0$ into Eq. (3.2), we obtain the variation of the shape energy in the form

$$\begin{aligned}\delta F = F - F_b^{(0)} = {} & \Delta p V_0 + \lambda A_0 + \oint [\Delta p - 2\lambda c_0(x+\tfrac{1}{2})] q dA \\ & + k \oint \Big\{ q^2 c_0^4 [2c_0^{-2}\rho^{-2} - 2x^3 - 4x^2 + \tfrac{1}{2} \\ & - (\Delta p/kc_0^3)(x+\tfrac{1}{2}) + (\lambda/kc_0^2)x(x+1)] \\ & + q_s^2 c_0^2 \Big[\tfrac{1}{2}\, c_0^{-2}\rho^{-2} - x^2 - \frac{x}{2} - 1 + (\lambda/2kc_0^2) \Big] \\ & + q_\phi^2 c_0^4 [c_0^{-2}\rho^{-2} - 2c_0^{-4}\rho^{-4} + (\lambda/2kc_0^2)c_0^{-2}\rho^{-2}] \\ & + \tfrac{1}{2}q_{ss}^2 + \tfrac{1}{2}q_{\phi\phi}^2\rho^{-4} + q_{s\phi}^2\rho^{-2} \Big\} dA. \end{aligned} \tag{3.17}$$

The above equation includes the first and the second variations of the shape energy with respect to $q(s,\phi)$ that describes the shape deformation normal to the equilibrium surface induced by the increase in the osmotic pressure difference and in the surface tension from zero to Δp and from zero to λ, respectively. Thus, Eq. (3.17) is the basic formula for the study of the instability and deformation of the vesicles.

IV. POLYGONAL SHAPE TRANSITION

A deformed shape should be an equilibrium one at which δF in Eq. (3.17) is minimum. In general, this minimization of δF with respect to $q(s,\phi)$ can be carried out using the well-known Euler-Lagrange approach; Eq. (3.17) can be rewritten as a Lagrangian integral

$$\delta F = \int L(q(s,\phi), q_s, q_{ss}, q_{s\phi}, q_\phi, q_{\phi\phi}) ds\, d\phi, \tag{4.1}$$

and then the Euler-Lagrange equation is

$$\frac{\partial L}{\partial q} - \frac{\partial}{\partial s}\frac{\partial L}{\partial q_s} - \frac{\partial}{\partial \phi}\frac{\partial L}{\partial q_\phi} + \frac{\partial^2}{\partial s \partial \phi}\frac{\partial L}{\partial q_{s\phi}} + \frac{\partial^2}{\partial s^2}\frac{\partial L}{\partial q_{ss}} + \frac{\partial^2}{\partial \phi^2}\frac{\partial L}{\partial q_{\phi\phi}} = 0, \tag{4.2}$$

where

$$\frac{\partial L}{\partial q} = 2k\rho c_0^4 (2c_0^{-2}\rho^{-2} - 2x^3 - 4x^2 + \tfrac{1}{2})q + \Delta p \rho - 2\Delta p \rho c_0 (x+\tfrac{1}{2})q - 2\lambda \rho c_0 (x+\tfrac{1}{2}) + 2\lambda \rho c_0^2 x(x+1)q, \tag{4.3}$$

$$\frac{\partial L}{\partial q_\phi} = [2k\rho c_0^4 (c_0^{-2}\rho^{-2} - 2c_0^{-4}\rho^{-4}) + \lambda \rho^{-1}] q_\phi, \tag{4.4}$$

$$\frac{\partial L}{\partial q_{s\phi}} = 2k\rho^{-1} q_{s\phi}, \tag{4.5}$$

$$\frac{\partial L}{\partial q_{ss}} = k\rho q_{ss}, \tag{4.6}$$

and

$$\frac{\partial L}{\partial q_{\phi\phi}} = k\rho^{-3} q_{\phi\phi} \tag{4.7}$$

can be obtained from Eq. (3.17). Equation (4.2) is a linear partial differential equation for $q(s,\phi)$. From Eqs. (4.3)–(4.7), we find that the general form of the solution $q(s,\phi)$ is

$$q(s,\phi) = \sum_{m=0}^{\infty} f_m(s) \cos m\phi, \tag{4.8}$$

where $f_m(s)$ satisfies some linear fourth-order ordinary differential equations. It is obvious that Eq. (4.8) exhibits the feature of the polygonal shape of the vesicle; however, there are no conventional methods to solve a fourth-order linear differential equation in general. For the present case, the numerical analyses of the differential equations are also difficult, because they cannot provide a clear and complete behavior of the solution. For these reasons, we use an approximate but very efficient approach to solve this problem.

Instead of solving the differential equations for $f_m(s)$, we assume the approximate solution of $q(s,\phi)$,

$$q = \rho^2 \beta(\phi), \tag{4.9}$$

where ρ^2 in the above solution is determined by analyzing the so-called index equations associated with the differential equations for $f_m(s)$; the solution can remove the singularity of δF in Eq. (3.17).

Using Eq. (4.9), Eq. (4.1) is reduced to the Lagrangian integral with respect to $\beta(\phi)$,

$$\delta F = \int_0^{2\pi} L(\beta, \beta_\phi, \beta_{\phi\phi}) d\phi, \tag{4.10}$$

where $\beta_\phi=(d/d\phi)\beta$ and $\beta_{\phi\phi}=(d/d\phi)\beta_\phi$. Substituting Eq. (4.9) into Eq. (3.17) and neglecting the two constant terms, ΔpV_0, and λA_0, we have an expression for $L(\beta,\beta_\phi,\beta_{\phi\phi})$ as

$$\begin{aligned}L=\int_0^{\rho_c}\{&2\lambda[-2\rho^2c_0(x+\tfrac{1}{2})\beta+\tfrac{1}{2}(4\rho^2\cos^2\psi\beta^2+\rho^2\beta_\phi^2)\\&+\rho^4c_0^2x(x+1)\beta^2]+\Delta p[2\rho^2\beta-\rho^4c_0(2x+1)\beta^2]\\&+2k[4-c_0^2\rho^2(2+6x+14x^2)\\&+c_0^4\rho^4(\tfrac{1}{2}+2x^2+8x^3+12x^4)]\beta^2\\&+2k[2+c_0^2\rho^2(1-4x^2)]\beta_\phi^2+k\beta_{\phi\phi}^2\}\frac{\rho}{\cos\psi}\,d\rho.\end{aligned}\tag{4.11}$$

We have used the basic relations given in the preceding sections, such as Eqs. (2.6), (3.3), and (3.4), in deducing the above equation. The Euler-Lagrange equation, Eq. (4.2), is then reduced to

$$\begin{aligned}&\Delta pw_1-c_0\lambda w_2+[\lambda(w_3+c_0^2z_2)-\Delta pc_0z_1+kA_1]\beta\\&\quad-(\lambda w_1+kA_2)\beta_{\phi\phi}+k\overline{A_0}\beta_{\phi\phi\phi\phi}=0,\end{aligned}\tag{4.12}$$

where $\beta_{\phi\phi\phi\phi}=d^4\beta/d\phi^4$, and w_1, w_2, w_3, z_1, z_2, $\overline{A_0}$, A_1, and A_2 have been obtained as

$$w_1=2\int_0^{\rho_c}(\rho^3/\cos\psi)d\rho=155\ \ \mu\mathrm{m}^4,\tag{4.13}$$

$$w_2=4\int_0^{\rho_c}[\rho^3(x+\tfrac{1}{2})/\cos\psi]d\rho=239\ \ \mu\mathrm{m}^4,\tag{4.14}$$

$$w_3=8\int_0^{\rho_c}\rho^3\cos\psi d\rho=352\ \ \mu\mathrm{m}^4,\tag{4.15}$$

$$z_1=4\int_0^{\rho_c}[\rho^5(x+\tfrac{1}{2})/\cos\psi]d\rho=2.85\times10^3\ \ \mu\mathrm{m}^6,\tag{4.16}$$

$$z_2=4\int_0^{\rho_c}[\rho^5x(x+1)/\cos\psi]d\rho=1.63\times10^3\ \ \mu\mathrm{m}^6,\tag{4.17}$$

$$\overline{A_0}=2\int_0^{\rho_c}(\rho/\cos\psi)d\rho=18.5\ \ \mu\mathrm{m}^2,\tag{4.18}$$

$$\begin{aligned}A_1=4\int_0^{\rho_c}\{&\rho[4-c_0^2\rho^2(2+6x+14x^2)\\&+c_0^4\rho^4(\tfrac{1}{2}+2x^2+8x^3+12x^4)]/\cos\psi\}d\rho\\=&81.0\ \ \mu\mathrm{m}^2.\end{aligned}\tag{4.19}$$

$$A_2=4\int_0^{\rho_c}\{\rho[2+c_0^2\rho^2(1-4x^2)]/\cos\psi\}d\rho=116\ \ \mu\mathrm{m}^2,\tag{4.20}$$

by using the geometrical parameters of RBCs described in Sec. II as those of the initial biconcave shape.

For the further calculation of the polygonal shape transformation, we put

$$\beta=\beta_0+\beta_m\cos m\phi.\tag{4.21}$$

Substituting Eq. (4.21) into the Euler-Lagrange equation Eq. (4.12), we have

$$\Delta pw_1-\Delta pc_0z_1\beta_0-c_0\lambda w_2+\lambda(w_3+c_0^2z_2)\beta_0+kA_1\beta_0=0,\tag{4.22}$$

$$\begin{aligned}&\{kA_1-\Delta pc_0z_1+\lambda(w_3+c_0^2z_2)\}\beta_m\cos m\phi\\&\quad+(\lambda w_1+kA_2)m^2\beta_m\cos m\phi+k\overline{A_0}m^4\beta_m\cos m\phi=0.\end{aligned}\tag{4.23}$$

Equation (4.22) gives the Lagrange multiplier λ as

$$\lambda=\frac{\Delta pw_1-\Delta pc_0z_1\beta_0+kA_1\beta_0}{c_0w_2-(w_3+c_0^2z_2)\beta_0}.\tag{4.24}$$

This equation shows the relation between the osmotic pressure difference and the surface tension in the shape deformation. With this result and Eq. (4.23), we obtain the most important relation,

$$\overline{\Delta p}\equiv-\frac{\Delta p}{kc_0^3}=\frac{(\overline{A_0}m^4+A_2m^2)[c_0w_2-(w_3+c_0^2z_2)\beta_0]+A_1(c_0w_2+m^2w_1\beta_0)}{c_0^3w_1(w_3+m^2w_1)+c_0^5(w_1z_2-z_1w_2)-c_0^4z_1w_1m^2\beta_0},\tag{4.25}$$

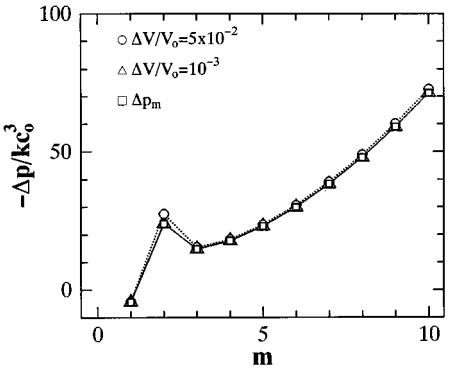

FIG. 4. Osmotic pressure difference for mth polygonally deformed vesicles at $\Delta V/V_0=5\times10^{-2}$ and 10^{-3}. The threshold pressure difference Δp_m is also shown. Here we take $-kc_0^3$ as the unit of pressure.

where $\overline{\Delta p}=-\Delta p/kc_0^3$ is the dimensionless osmotic pressure difference ($\overline{\Delta p}$ is positive because of $c_0<0$). From the conservation of area,

$$\delta A=\int d\phi\int \frac{2\rho}{\cos\psi}\{-2\rho^2c_0(x+\tfrac{1}{2})(\beta_0+\beta_m\cos m\phi) +\tfrac{1}{2}\,[4\rho^2\cos^2\psi(\beta_0+\beta_m\cos m\phi)^2+m^2\rho^2\beta_m^2\sin^2 m\phi] +c_0^2\rho^4x(x+1)(\beta_0+\beta_m\cos m\phi)^2\}d\rho=0 \tag{4.26}$$

and Eqs. (4.13)–(4.20), we obtain

$$-4w_2c_0\beta_0+2w_3(\beta_0^2+\tfrac{1}{2}\beta_m^2)+m^2w_1\beta_m^2+2c_0^2z_2\beta_0^2 +c_0^2z_2\beta_m^2=0, \tag{4.27}$$

which permits us to determine β_0 as

$$\beta_0=\beta_m^2(w_3+m^2w_1+c_0^2z_2)/4w_2c_0, \tag{4.28}$$

where we neglect the terms of β_0^2. This equation is used to numerically analyze the polygonal shape transformation, and it is obvious that for $c_0<0$, β_0 is always negative, showing that the shape transformation is the compressive process of the vesicle. We note that Eq. (4.28) is only valid for a small deformation of the vesicle.

V. DISCUSSION

First we discuss the threshold osmotic pressure difference for the polygonal shape transformation. The shape transformation occurs above the threshold osmotic pressure difference

$$\Delta p_m=(-kc_0^3)\,\frac{w_2(m^4\overline{A_0}+m^2A_2+A_1)}{c_0^2w_1(m^2w_1+w_3)+c_0^4(w_1z_2-z_1w_2)} \qquad (m=1,2,3,\ldots), \tag{5.1}$$

which is obtained from Eq. (4.25) by putting $\beta_0=0$, because at the threshold both β_0 and β_m are zero. Using the numerical values in Eqs. (4.13)–(4.20), we can calculate Eq. (5.1) for $m=1,2,...,10$ and show the results in Fig. 4. The threshold osmotic pressure difference is a monotonic increasing function of m except for $m=2$. It is interesting to note that in the case of the polygonal shape deformation of a spherical vesicle induced by pressure [17,19], the threshold pressure exhibits a monotonic increase with m as well.

Hotani [7] has experimentally shown that the increase in the concentration of a variety of reagents such as NaCl, KCl, and $CaSO_4$ causes the polygonal shape transition of the biconcave liposomes. From the van't Hoff law [27], the osmotic pressure difference across a membrane separating two ideal, dilute solutions can be related to the concentration difference of the solutions as

$$\Delta p=p_{\rm out}-p_{\rm in}=RT(c_{\rm out}-c_{\rm in})=RT\Delta c, \tag{5.2}$$

where R is the universal gas constant and T is the temperature. It is obvious that the increase in $c_{\rm out}$ increases Δp. This finding is consistent with the present theoretical prediction; however, Hotani has observed only elliptical, triangular, square, and pentagonal shapes, which correspond to $m=2$, 3, 4, and 5, [see Figs. 2(b)–2(e) in Ref. [7] as well as Fig. 1]. The reason why the vesicle with $m=1$, whose shapes are shown in Fig. 5(a), has not been observed is that the threshold pressure difference for $m=1$ is negative in the present calculation, as shown in Fig. 4. In addition, the reason why deformed liposomes having $m>5$ have not been observed is that the threshold pressure lies between Δp_5 and Δp_6 in Hotani's experiment. It is therefore expected that the liposomes having $m>5$ will be observable above $\Delta p>\Delta p_5$. The experimental confirmation of this prediction will be an interesting issue in the future.

Next, we discuss the development of the shape deformations above the threshold pressure Δp_m. For this purpose, we calculate the compressive ratio of the volume of the vesicle, $\Delta V/V_0$. In the linear approximation, $\Delta V/V_0$ can be obtained as

$$\frac{\Delta V}{V_0}=\frac{\oint qdA}{V_0} =\frac{2}{V_0}\int_0^{2\pi}d\phi\int_0^{\rho_c}\frac{\rho^3}{\cos\psi}\,(\beta_0+\beta_m\cos m\phi)d\rho =\left(\frac{2\pi}{V_0}\right)w_1\beta_0, \tag{5.3}$$

where w_1 is given by Eq. (4.13). The top view of a mth polygonally deformed vesicle is calculated using Eqs. (4.9) and (4.21) and is given by

$$\rho=\rho_c+\rho_c^2(\beta_0+\beta_m\cos m\phi). \tag{5.4}$$

In Fig. 5, we show the development of the top view of the deformed vesicles for $m=1$ to 5 at some $\Delta V/V_0$ values. The corresponding Δp values are also shown in the figure, which are computed from Eq. (4.25). We find that in a mode of m, Δp slightly increases with increasing $|\Delta V/V_0|$, as shown in Figs. 4 and 5. This behavior is consistent with the experiment [7].

The agreement between the theory presented above and the experiment [7] shows that the basic approximation for

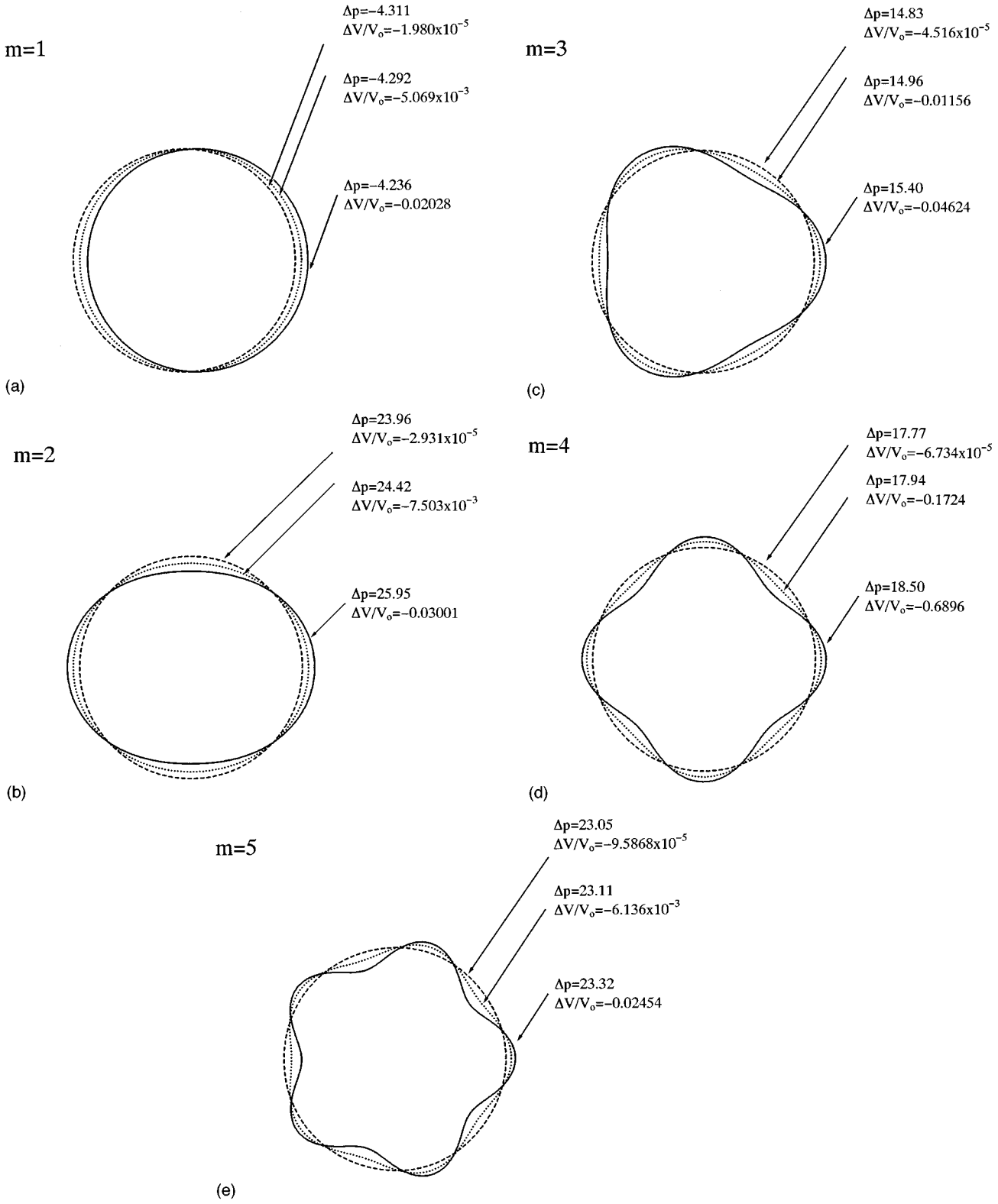

FIG. 5. Top views of circular biconcave vesicles with several polygonal deformations; (a) asymmetric shape ($m=1$), (b) elliptical shape ($m=2$), (c) triangular shape ($m=3$), (d) square shape ($m=4$), and (e) pentagonal shape ($m=5$) as a function of the osmotic pressure differences in units of $-kc_0^3$ and the ratio of the change in the volume, $\Delta V/V_0$.

$q(\rho,\phi)$ in Eq. (4.9) is reasonable. Equation (4.9) states that the deformation from the initial biconcave shape quadratically increases with increasing distance from the center of the vesicle, ρ. This leads to the fact that the side view of the vesicle is maintained in the circular biconcave shape, as observed in the experiment.

Here, we would like to comment on the previous theoretical analysis for the polygonal shape transformation by

Sekimura and Hotani [8]. They have employed the Canham model, which is a special case of the Helfrich spontaneous curvature model ($c_0=0$), have not considered the effect of the osmotic pressure difference, and have used the modified Cassini equation, which is not a solution of the shape equa tion for axisymmetric vesicles, Eq. (2.4). We thereby point out that their theoretical results cannot be directly compared with the experimental results of Hotani [7]. For example, Sekimura and Hotani have shown that only the vesicles with $m=2$ deformation have the minimum shape energy at $\Delta V/V_0 \sim 10^{-3}$. On the other hand, in our present calculation, all experimentally observed deformations with $m=2$–5 are found at the same $\Delta V/V_0$. Furthermore, they have not given the result of the $m=5$ deformation, which has been observed in the experiment [7].

Finally, we briefly discuss the other shapes of liposomes found in the experiment [7] that have not been explained in the present calculation. For example, the strongly deformed shape for $m=2$ is a peanutlike or a dumbbell-like form [Fig. 2(f) in Ref. [7]] and further grows to become a cylinder [Fig. 2(l) in Ref. [7]]. For the description of such a process, the present calculation, based on up to the second variation of the shape energy, is not suitable, because the expression for the shape energy is valid only for small deformations. However, we stress that a peanutlike or dumbbell-like vesicle can be described by the solution of Eq. (2.10) in the case of $c_0>0$. In a recent paper [25], it has been shown that there exists a relation between c_0 and the membrane potential U_M,

$$c_0=\frac{e_{11}U_M}{k}+c_0^{(0)}, \tag{5.5}$$

where $c_0^{(0)}$ takes account of the asymmetric distribution of the molecules in the bilayer, $e_{11}\simeq 10^{-4}$ dyne$^{1/2}$ [28] is the piezoelectric constant of the membrane, and the membrane potential U_M is defined as

$$U_M=U_{\rm in}-U_{\rm out}. \tag{5.6}$$

According to the Nernst equilibrium equation [27], we have

$$U_M=\frac{RT}{z\mathcal{F}}\ln\left(\frac{c_{\rm out}}{c_{\rm in}}\right), \tag{5.7}$$

where z is the valence of the ions in the solutions and $\mathcal{F}$ is the Faraday constant. We find from Eq. (5.2) that at the initial state of the liposomes, $c_{\rm out}$ is equal to $c_{\rm in}$ for $\Delta p=0$, but with increasing Δp, $c_{\rm out}$ becomes larger than $c_{\rm in}$, which leads to $c_0>0$, as evident from Eqs. (5.5) and (5.7). Since cylindrical vesicles have $c_0>0$ [17], c_0 is another driving force of the cylinder formation process. From this discussion, we suggest that for the analysis of the large deformations shown in Figs. 2(l)–(z) in Ref. [7], the changes in c_0 as well as Δp must be considered simultaneously.

VI. CONCLUSIONS

We have analyzed the polygonal shape transformation observed in liposomes on the basis of the Helfrich spontaneous curvature model. We show that the analytical solution of the shape equation for axisymmetric vesicles represents a circular biconcave discoid for $c_0<0$, and thus use the solution as an initial biconcave shape. We then calculate the shape energy of the deformed vesicles by taking account of up to the second variation. From the minimization of the shape energy in terms of the Euler-Lagrange approach, the threshold osmotic pressure difference for mth-polygonal deformation is derived and the shapes of the deformed vesicles are displayed as a function of the osmotic pressure and the change in the volume of the vesicles. We confirm the experimental evidence that the increase in the osmotic pressure is the driving force of the polygonal transformation. In the experiment, further transformation from the polygonal shapes to cylinder-like shapes has been observed as well. The present theory cannot be applied to the analysis of this transformation, because the theory is valid for small deformations of the vesicles from the biconcave shape. We therefore discuss a mechanism of the transformation to the cylinders, and indicate that the positive spontaneous curvature as well as the increase in the osmotic pressure are the driving force of the transformation.

ACKNOWLEDGMENTS

This work was supported by Advanced Research Foundation of Osaka Prefecture University. We would also like to thank Prof. Y. Kawakatu of Tokyo Metropolitan University for unpublished results.

[1] For a review, see for example, *Physics of Amphiphile Layers*, edited by J. Meunier, D. Langevan, and N. Boccara (Springer, Berlin, 1987).
[2] W. Helfrich and H. J. Deuling, J. Phys. (Paris) **36**, C1-327 (1975).
[3] W. W. Webb, Q. Rev. Biophys. **9**, 49 (1976).
[4] R. J. Nossal and H. Lecar, *Molecular and Cell Biophysics* (Addison Wesley, Redwood, CA, 1991).
[5] P. G. de Gennes and C. Taupin, J. Phys. Chem. **86**, 2294 (1982); S. A. Safran and L. A. Turkevich, Phys. Rev. Lett. **50**, 1930 (1983); B. Duplantier, Physica (Amsterdam) **168A**, 179 (1990).
[6] E. Evans and W. Rawicz, Phys. Rev. Lett. **64**, 2094 (1990).
[7] H. Hotani, J. Mol. Biol. **178**, 113 (1984).
[8] T. Sekimura and H. Hotani, J. Theor. Biol. **149**, 325 (1992).
[9] R. B. Canham, J. Theor. Biol. **26**, 61 (1970).
[10] E. A. Evans and Y. C. Fung, Microvasc. Res. **4**, 335 (1972).
[11] W. Helfrich, Z. Naturforsch. **28C**, 693 (1973).
[12] H. J. Deuling and W. Helfrich, Biophys. J. **16**, 861 (1976).
[13] T. Kawakatsu, D. Andelman, K. Kawasaki, and T. Taniguchi, J. Phys. (France) II **3**, 971 (1993).
[14] U. Seifert, Phys. Rev. Lett. **66**, 2404 (1991); U. Seifert, K. Berndl, and R. Lipowsky, Phys. Rev. A **44**, 1182 (1991); J. Berndl, J. Kas, R. Lipowsky, E. Sackmann, and U. Seifert, Europhys. Lett. **13**, 659 (1990).
[15] Hu Jian-Guo and Ou-Yang Zhong-can, Phys. Rev. E **47**, 461 (1993).

[16] C. Tanford, Proc. Natl. Acad. Sci. USA **76**, 3318 (1979).
[17] Ou-Yang Zhong-can and W. Helfrich, Phys. Rev. A **39**, 5280 (1989).
[18] S. Svetina and B. Zeks, Biomed. Biochim. Acta **42**, 86 (1983).
[19] Ou-Yang Zhong-can and W. Helfrich, Phys. Rev. Lett. **59**, 2486 (1987); a more general shape equation corresponding to a generalized Helfrich energy integrand has been derived by J. C. C. Nitsche in *Lectures on Minimal Surfaces* (Cambridge, 1989), Vol. I, p. 24; and in Q. Appl. Math. **51**, 363 (1993).
[20] H. Deuling and W. Helfrich, J. Phys. (Paris) **37**, 1335 (1976); J. Jenkins, J. Math. Biophys. **4**, 149 (1977); M. Peterson, J. Appl. Phys. **57**, 1739 (1985); S. Svetina and B. Zecks, Eur. Biophys. J. **17**, 101 (1989); L. Miao, B. Fourcade, M. Rao, M. Wortis, and R. K. P. Zia, Phys. Rev. A **43**, 6843 (1991); B. Fourcade, L. Miao, M. Rao, M. Wortis, and R. K. P. Zia, Phys. Rev. E **49**, 5276 (1994); L. Miao, U. Seifert, M. Wortis, and H. G. Döbereiner, *ibid*. **49**, 5389 (1994).
[21] F. Brochard and J. F. Lennon, J. Phys. (Paris) **36**, 1035 (1975).
[22] P. G. de Gennes, Rev. Mod. Phys. **64**, 645 (1992).
[23] H. Naito, M. Okuda, and Ou-Yang Zhong-can, Phys. Rev. E **48**, 2304 (1993).
[24] A. W. L. Jay, Biophys. J. **15**, 205 (1975).
[25] Ou-Yang Zhong-can, Hu Jian-Guo, and Liu Ji-xing, Mod. Phys. Lett. B **6**, 1577 (1992).
[26] J. J. Stoker, *Differential Geometry* (Wiley, New York, 1969).
[27] S. G. Schultz, *Basic Principles of Membrane Transport* (Cambridge University Press, London, 1980).
[28] D. Schmidt, M. Schadt, and W. Helfrich, Z. Naturforsch, **27A**, 277 (1972).